Heat-induced Transformations of Adsorbed Hydrocarbon Residues on Graphene

Benedikt Westenfelder

We describe new phenomena of structural reorganization of carbon adsorbates as revealed by in situ *atomic-resolution transmission electron microscopy (TEM) performed on specimens at extreme temperatures. In our investigations, a graphene sheet serves as both a quasi-transparent substrate for TEM and as an* in situ *heater. The melting of gold nanoislands deposited on the substrate surface is used to evaluate the local temperature. At annealing temperatures around 1000 K we observe the transformation of physisorbed hydrocarbon adsorbates into amorphous carbon monolayers and the initiation of crystallization. At temperatures exceeding 2000 K the transformation terminates in the formation of a completely polycrystalline graphene state. The resulting layers are bounded by free edges primarily in the armchair configuration.*

1. Introduction

The recent past has witnessed tremendous gains in the capabilities of transmission electron microscopy (TEM) for exploring the atomic configuration of materials, largely because of dramatic improvements in the correction of lens aberrations. It is now possible to obtain atomic-resolution images even of light-element materials, with a reduction in radiation damage effected by the utilization of reduced acceleration voltages (for more background info see ref. [1]). Our understanding of carbon systems, such as graphene or carbon nanotubes, has significantly benefitted from these instrumental developments. When a TEM is exploited as a platform for *in situ* experimentation, dynamic phenomena can be studied under direct observation of the atomic structure [2], but, owing to practical limitations, such investigations have been limited so far to temperatures below about 1500 K [3–5]. Our recent investigations enabled observations of heat-induced transformations of carbon adsorbates on a graphene substrate raised to temperatures in excess of 2000 K.

2. Experiment

In our experiments, a graphene sheet serves as both a quasi-transparent substrate for transmission electron microscopy and as an *in situ* heater that can withstand unprecedented temperatures [6] owing to its high mechanical [7, 8], thermal [6] and chemical stability. As reference points for the local temperature, we used the melting of gold particles (diameter dependent), the transition from amorphous to crystalline silicon nitride (1600 K) and the evaporation of SiN (2000 K) [9]. The experimental concept and thermal calibration have been described in greater detail previously [9]. In brief, a graphene sheet is transferred onto a Si/SiN membrane platform prestructured with windows and gold contacts, resulting in a TEM-compatible geometry providing an electrically contacted graphene substrate with a freestanding region for transmission of the electron beam Fig. (1). The graphene layer was studied by aberration-corrected high-resolution transmission electron microscopy (AC-HRTEM) performed by a TITAN (80-300) FEI microscope equipped with a Fischione 2510 biasing TEM holder and operated at an accelerating voltage of 80 kV. Electrical current was passed through graphene specimens by applying a voltage between the gold contacts of the sample platform, achieving a typical current density on the order of 2×10^7 A/cm^2 (assuming a graphene thickness of 0.34 nm per layer) at an applied bias of 2 V. The heat-induced transformations of gold nanoislands deposited on graphene by thermal evaporation reveal the local temperature of the substrate. In this letter we focus on the initial scientific results yielded by this experimental approach.

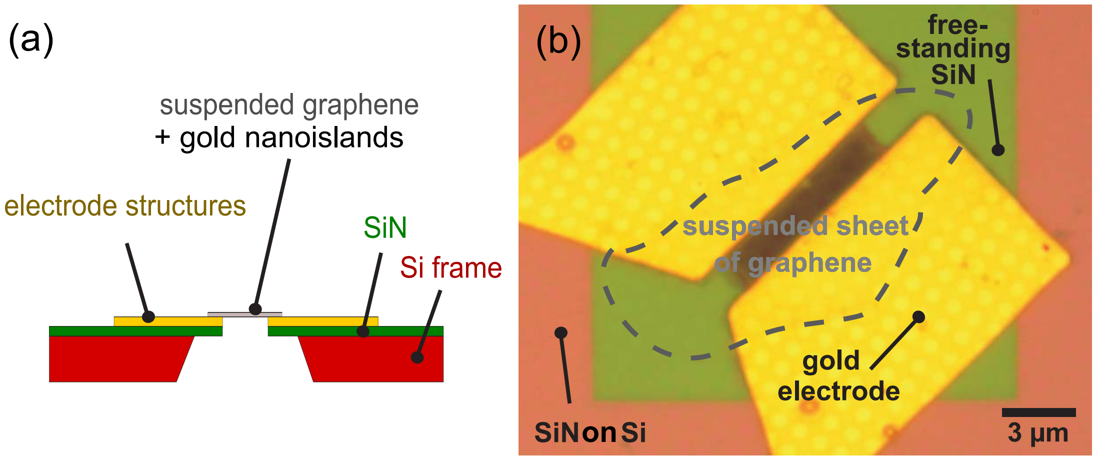

Fig. 1: (a) Cross-sectional schematic illustration of the sample carrier design. (b) Optical micrograph of the electrode support structure upon which a graphene sheet is suspended.

2.1 Temperature estimation during mild heating

Observations made during mild heating conditions help in the estimation of the temperature for our sample geometry [1, 9]. It is well known that the diffusion of Au adatoms on the surface of gold nanoparticles is significant even at room temperature (RT) [10, 11], leading to continuous shape changes of the particles upon heating [12]. In the case of gold nanoislands deposited on graphene, we were able to correlate a decrease in the particle surface area-to-volume ratio with an increase in temperature [1]. Above a certain temperature, the first particles form liquid drops and begin to evaporate [9, 13]. According to theoretical predictions and experimental findings, the melting temperature depends strongly on the particle size, with gold particles ranging in diameter from 3 to 20 nm expected to melt between 800 and 1300 K [14].

3. Observations in the Level of Individual Atoms

We now turn our attention to structural observations extending down to the level of individual atoms. Adsorbed hydrocarbon residues originating from the sample preparation undergo remarkable transformations at the atomic level when exposed to high temperatures. The use of a graphene substrate allows us to observe the precise atomic configuration of the carbon adsorbates. Moreover, graphene enables locally high temperatures to be reached while simultaneously providing a stable supporting surface that does not interact strongly with the adsorbates.

3.1 Hydrocarbon deposits at room temperature

A typical hydrocarbon deposit on an as-prepared graphene sample at 300 K is shown in Fig. 2a. Under electron irradiation at 80 kV, mobile hydrocarbon deposits are converted to amorphous carbon, while hydrogen atoms are knocked out by electron impacts.

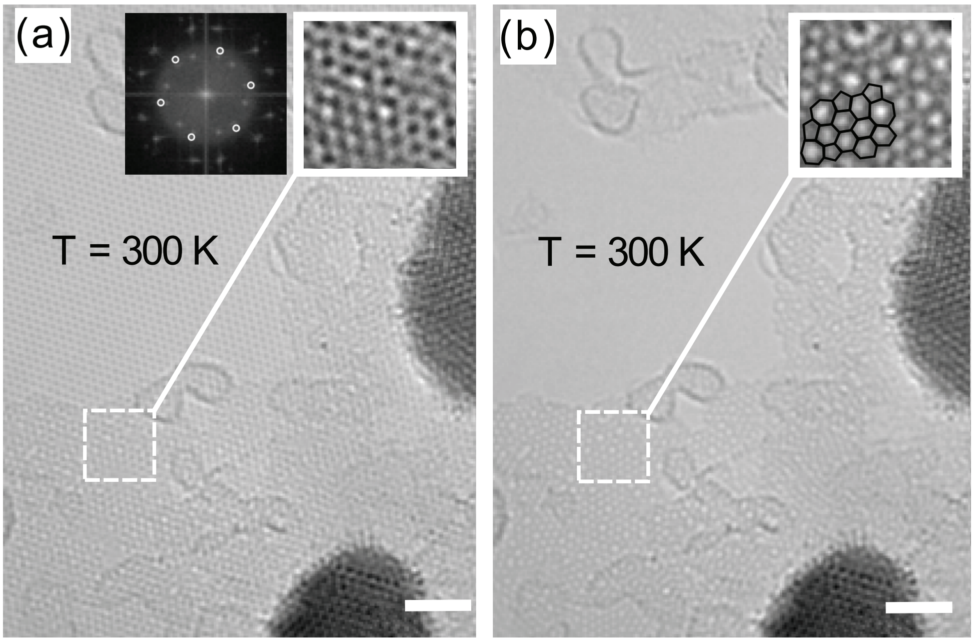

Fig. 2: AC-HRTEM images of carbon and hydrocarbon adsorbates (and gold nanoparticles) on graphene (scale bars = 2 nm). (a) Unfiltered image of carbon contamination and gold particles on a bilayer graphene substrate prior to heat treatment. The upper left inset shows an FFT of the entire image, containing diffraction peaks arising from the substrate (circled in white) and from gold. (b) Same image as in (a) after Fourier filtering of the graphene substrate. This procedure reveals the atomic structure of the amorphous carbon adsorbates, which is clearly resolved in the thinnest areas. The inset shows the region in the dashed box at higher magnification and contrast. The arrangement of atoms in the adsorbate can be interpreted as a random combination of carbon pentagons, hexagons and heptagons. The shape of the gold nanoislands (dark contrast at lower left and right) and their absence of encapsulating carbon shells indicate that the sample had not yet seen temperatures in excess of about 425 °C.

The resulting amorphous carbon adsorbates are comparably stable under further electron-beam irradiation, and they do not easily desorb at high temperatures. In the thinnest regions, we can even resolve the atomic structure of the adsorbates (Fig. 2b), which appears to be amorphous, consisting of a seemingly random arrangement of carbon pentagons, hexagons, heptagons and other (less-frequently observed) carbon polygons.

3.2 Transformations at moderate temperatures (≈1000 K)

The situation changes, however, when we apply temperatures of ≈ 1000 K (indicated by partial melting of the gold particles) at a heating current of $2 \times 10^7\,\mathrm{A/cm^2}$. First, the adsorbates reorganize into structures characterized by large areas consisting of single-layer amorphous carbon containing some crystallized domains (Fig. 3). Second, gold atoms originating from the surrounding nanoislands are incorporated into the carbon matrix, as marked by the arrows in Fig. 3b. Our AC-HRTEM images taken at 1000 K appear to be similar to those obtained by Turchanin et al. [15] from annealed samples characterized at RT—i.e., both crystalline and amorphous domains are observed.

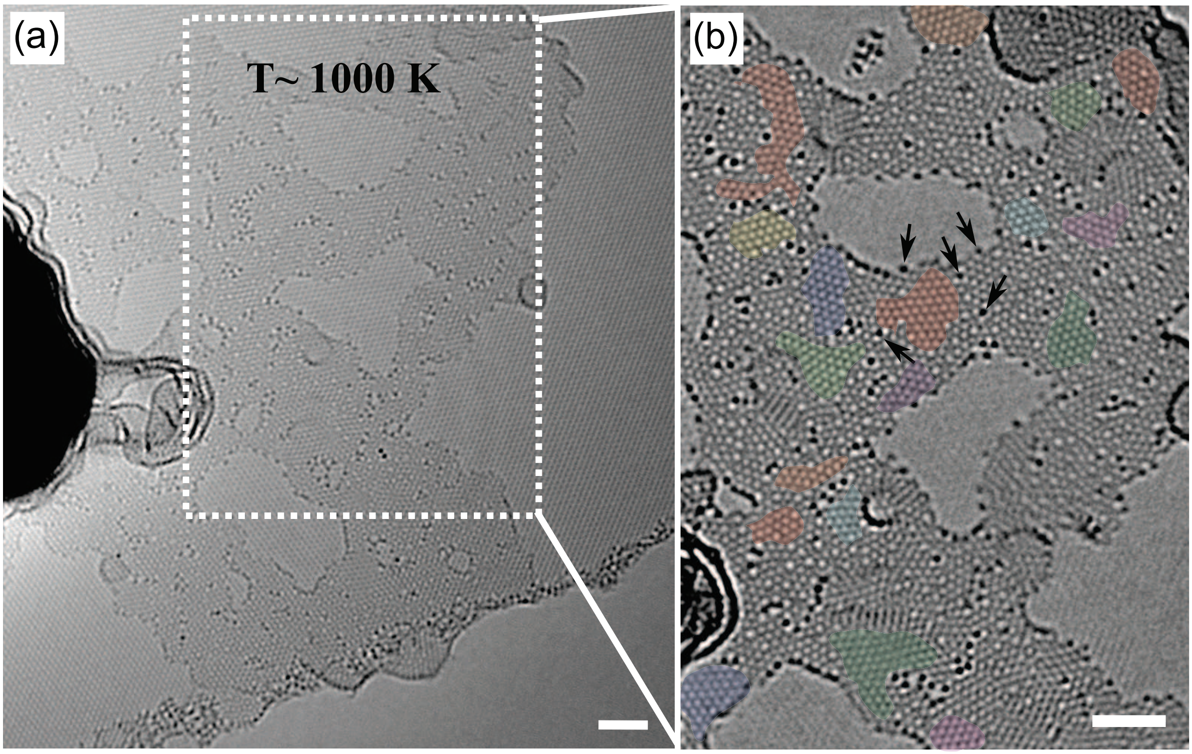

Fig. 3: (a) AC-HRTEM image of single-layer carbon adsorbates on a graphene substrate at 1000 K. (b) Fourier-filtered and magnified region from (a): here, crystalline domains (shaded in color) are evident in some regions, whereas others are still amorphous. Many edge sites and vacancies are occupied by individual gold atoms (black spots, several indicated by arrows). Scale bars are 2 nm in length.

3.3 Transformations at extreme temperatures ($\approx 2000\,\mathrm{K}$)

When we raise the temperature to approximately 2000 K (the heating current is now increased by a factor of two, and silicon nitride close to the imaged region begins to sublimate), the adsorbate transformation ends in fully crystallized graphene domains separated only by atomically sharp boundaries (Fig. 4a). In other words, the amorphous carbon contamination has been transformed almost completely into a polycrystalline graphene layer situated on top of the existing graphene substrate. Image pairs 1 to 3 in Fig. 4b illustrate various dynamic rearrangements of carbon bonds that occur at the grain boundaries, leading to greater crystallinity. The thermally induced healing of defect-like vacancies inside a crystalline grain is captured in image pair 4 of Fig. 4b. We observe a polycrystalline graphene sheet having a domain size of 1 to 3 nm lying on top of a defect-free crystalline graphene substrate (Fig. 4a). Some of the adsorbate grains are aligned with the underlying graphene lattice; however, other crystalline domains appear to be randomly oriented. Owing to the small domain size, we obtain a large number of grain boundaries within the field of view of the AC-HRTEM image. In agreement with previous studies by other authors [16, 17], we find that the grain boundaries consist of carbon pentagons and heptagons arranged in such a manner as to connect adjacent domains of differing orientation without dangling bonds.

Since the polycrystalline adsorbate layer does not completely cover the underlying substrate, we are able to observe a large number of "free edges" of individual grains. In contrast to previous room-temperature HRTEM observations of beam-induced holes in graphene [18,19], these edges are formed and observed under high-temperature annealing. Most strikingly, most of the annealed edges exhibit an armchair-type configuration (Fig. 4c). The contrast at the edges is in agreement with the presence of carbon atoms; the slightly stronger contrast of the edge atoms compared to the lattice in Fig. 4 is a result of the contrast transfer function (CTF) of the microscope at the present conditions. In a statistical analysis of the edge configurations (see Ref. [1]), 58 % of all visible edges could be assigned clearly to one of the geometries calculated in Ref. [20]. Among the classified edges, a dominant fraction —83 %— exhibits the armchair conformation, 14 % manifest the 5–7 reconstructed zigzag edge structure, and only 3 % are found in the unreconstructed zigzag geometry.

These observations are in excellent agreement with expectations from theory (Table 1 in Ref. [20]): The unreconstructed armchair edge and the 5–7 reconstructed zigzag are the two lowest-energy edge configurations. In light of these calculations, it is surprising that AC-HRTEM characterizations of freestanding graphene samples at room temperature [18, 19] observed a slight preponderance of the unreconstructed zigzag configuration, especially since the energy of the latter is 0.33 eV/Å (or 1.1 eV per atom) higher than that of the armchair edge [20]. It has been speculated previously that this finding arises from the unreconstructed zigzag edges being less sensitive to radiation damage [18]. In the case of high-temperature annealing, however, the thermodynamically preferred armchair configuration appears to be most stable, as observed not only in our measurements but also in recent investigations performed by Song et al. [22].

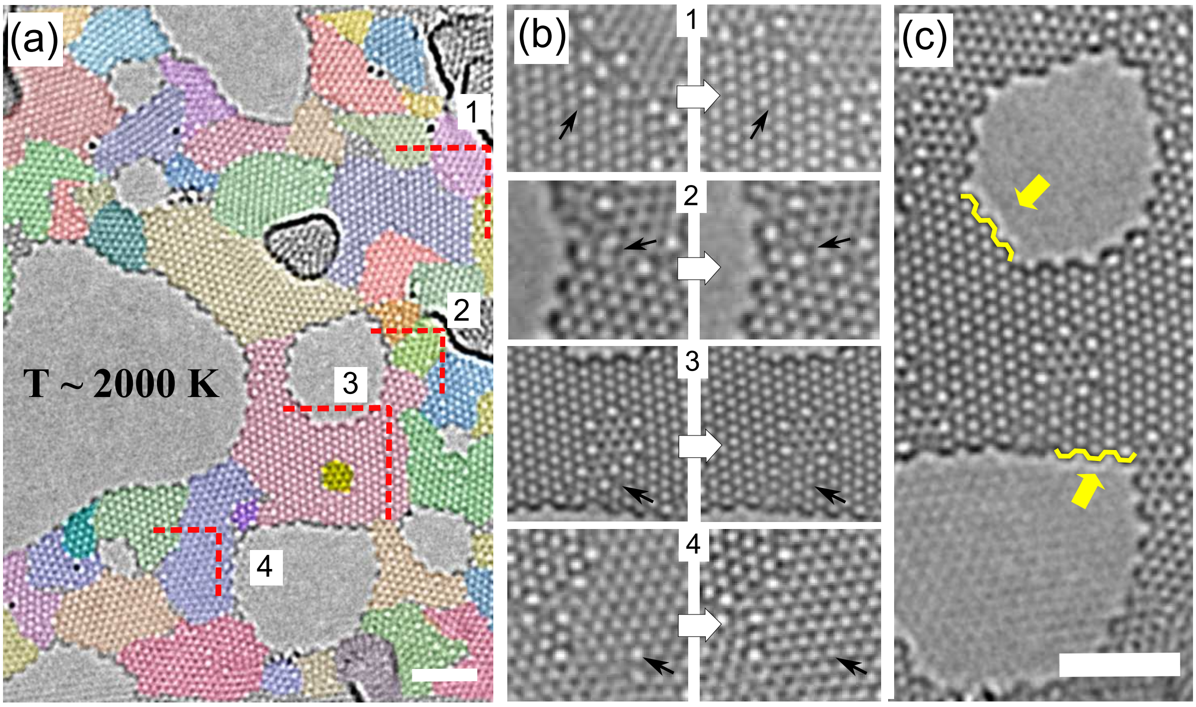

Fig. 4: (a) Fourier-filtered micrograph showing fully developed grains (shaded in color) of graphene. The filtering procedure worked perfectly only in the central part of the image. This micrograph was recorded during extreme heat treatment above 2000 K, as estimated from the behavior of freestanding SiN located close to the sample (amorphous SiN is known to crystallize at 1600 K [21] and to begin decomposing around 2000 K [9]). (b) Numbered image pairs capturing dynamic rearrangements of carbon bonds during constant heating (left image = starting configuration; right image = after 100 s). (c) Markers indicate armchair-type atomic configurations at the free edges of adsorbate layers. Scale bars are 2 nm in length.

4. Conclusions

In summary, we have presented atomically resolved *in situ* TEM studies of the heat-induced evolution of hydrocarbons on graphene. Temperature profiles with maxima up to ≈ 2000 K were obtained by passing an electrical current through a freestanding graphene substrate. We found that extreme heat activates a transformation of adsorbed hydrocarbons on top of graphene into atomic monolayers of amorphous carbon, followed by crystallization. The resulting polycrystalline layers consist of free edges showing predominantly armchair configuration.

Acknowledgment

We thank our technicians Ilona Argut, Susanne Menzel, Rudolf Rösch, Rainer Blood and Yakiv Men for their technical support. A special thank goes to Prof. Dr. Jannik C. Meyer for his collaboration with respect to scientific questions and the microscope operation.

References

[1] B. Westenfelder, J.C. Meyer, J. Biskupek, S. Kurasch, F. Scholz, C.E. Krill, and U. Kaiser, "Transformations of carbon adsorbates on graphene substrates under extreme heat", *Nano Lett.*, vol. 11, pp. 5123–5127, 2011.

[2] F.M. Ross, "In situ transmission electron microscopy", in *Science of Microscopy*, P.W. Hawkes and J.C.H. Spence (Eds.), pp. 445–534, Springer New York, 2007.

[3] T. Kamino, T.Y. Takahiro Sato, and T. Hashimoto, "Development of a technique for high resolution electron microscopic observation of nano-materials at elevated temperatures", *J. Electron Microsc.*, vol. 54, pp. 505–508, 2005.

[4] P.L. Gai and E.D. Boyes, "A very high temperature (2000 °C) stage for atomic resolution *in situ* ETEM", in *EMC 2008 14th European Microscopy Congress 1–5 September 2008, Aachen, Germany*, M. Luysberg, K. Tillmann, and T. Weirich (Eds.), pp. 481–482, Springer Berlin Heidelberg, 2008.

[5] A. Mayoral, L.F. Allard, D. Ferrer, R. Esparza, and M. Jose-Yacaman, "On the behavior of Ag nanowires under high temperature: in situ characterization by aberration-corrected STEM", *J. Mater. Chem.*, vol. 21, pp. 893–898, 2011.

[6] K. Kim, W. Regan, B. Geng, B. Alemán, B.M. Kessler, F. Wang, M.F. Crommie, and A. Zettl, "High-temperature stability of suspended single-layer graphene", *Phys. Status Solidi (RRL)*, vol. 4, pp. 302–304, 2010.

[7] C. Lee, X. Wei, J.W. Kysar, and J. Hone, "Measurement of the elastic properties and intrinsic strength of monolayer graphene", *Science*, vol. 321, pp. 385–388, 2008.

[8] T.J. Booth, P. Blake, R.R. Nair, D. Jiang, E.W. Hill, U. Bangert, A. Bleloch, M. Gass, K.S. Novoselov, M.I. Katsnelson, and A.K. Geim, "Macroscopic graphene membranes and their extraordinary stiffness", *Nano Lett.*, vol. 8, pp. 2442–2446, 2008.

[9] B. Westenfelder, J.C. Meyer, J. Biskupek, G. Algara-Siller, L.G. Lechner, J. Kusterer, U. Kaiser, C.E. Krill III, E. Kohn, and F. Scholz, "Graphene-based sample supports for in situ high-resolution TEM electrical investigations", *J. Phys. D: Appl. Phys.*, vol. 44, pp. 055502-1–7, 2011.

[10] J.O. Bovin, R. Wallenberg, and D.J. Smith, "Imaging of atomic clouds outside the surfaces of gold crystals by electron microscopy", *Nature*, vol. 17, pp. 47–49, 1985.

[11] S. Iijima and T. Ichihashi, "Motion of surface atoms on small gold particles revealed by HREM with real-time VTR system", *Jpn. J. Appl. Phys.*, vol. 24, pp. L125–L128, 1985.

[12] E. Sutter, P. Sutter, and Y. Zhu, "Assembly and interaction of Au/C core-shell nanostructures: in situ observation in the transmission electron microscope", *Nano Lett.*, vol. 5, pp. 2092–2096, 2005.

[13] A.S. Barnard, N.P. Young, A.I. Kirkland, M.A. van Huis, and H. Xu, “Nanogold: a quantitative phase map”, *ACS Nano*, vol. 3, pp. 1431–1436, 2009.

[14] P. Buffat and J.P. Borel, “Size effect on the melting temperature of gold particles”, *Phys. Rev. A*, vol. 13, pp. 2287–2298, 2000.

[15] A. Turchanin, D. Weber, M. Büenfeld, C. Kisielowski, M.V. Fistul, K.B. Efetov, T. Weimann, R. Stosch, J. Mayer, and A. Gölzhäuser, “Conversion of self-assembled monolayers into nanocrystalline graphene: structure and electric transport”, *ACS Nano*, vol. 5, pp. 3896–3904, 2011.

[16] P.Y. Huang, C.S. Ruiz-Vargas, A.M. van der Zande, W.S. Whitney, M.P. Levendorf, J.W. Kevek, S. Garg, J.S.A.C.J. Hustedt, Y. Zhu, J. Park, P.L. McEuen, and D.A. Muller, “Grains and grain boundaries in single-layer graphene atomic patchwork quilts”, *Nature*, vol. 469, pp. 389–392, 2011.

[17] O.V. Yazyev and S.G. Louie, “From graphene constrictions to single carbon chains”, *Nature Materials*, vol. 9, pp. 806–809, 2010.

[18] C.O. Girit, J.C. Meyer, R. Erni, M.D. Rossell, C. Kisielowski, L. Yang, C.H. Park, M.F. Crommie, M.L. Cohen, S.G. Louie, and A. Zettl, “Graphene at the edge: stability and dynamics”, *Science*, vol. 323, pp. 1705–1708, 2009.

[19] A. Chuvilin, J.C. Meyer, G. Algara-Siller, and U. Kaiser, “From graphene constrictions to single carbon chains”, *New J. Phys.*, vol. 11, pp. 083019-1–10, 2009.

[20] P. Koskinen, S. Malola, and H. Häkkinen, “Self-passivating edge reconstructions of graphene”, *Phys. Rev. Lett.*, vol. 101, pp. 115502-1–4, 2008.

[21] Y. Li, Y. Liang, F. Zheng, X. Shong, and Z. Hu, “Phase transition and particulate growth of laser synthesized ultrafine amorphous silicon nitride powders”, *J. Mater. Sci. Lett.*, vol. 13, pp. 1588–1590, 1994.

[22] B. Song, G.F. Schneider, Q. Xu, G. Pandraud, C. Dekker, and H. Zandbergen, “Atomic-scale electron-beam sculpting of near-defect-free graphene nanostructures”, *Nano Lett.*, vol. 11, pp. 2247–2250, 2011.